

Energy Advances

Accepted Manuscript

This article can be cited before page numbers have been issued, to do this please use: F. Muhammad, J. J. Nisar, G. Ali, F. Anwar, W. A. Wan Abdul Karim Ghani, A. Sharif and E. Ahmed, *Energy Adv.*, 2025, DOI: 10.1039/D4YA00600C.



This is an Accepted Manuscript, which has been through the Royal Society of Chemistry peer review process and has been accepted for publication.

Accepted Manuscripts are published online shortly after acceptance, before technical editing, formatting and proof reading. Using this free service, authors can make their results available to the community, in citable form, before we publish the edited article. We will replace this Accepted Manuscript with the edited and formatted Advance Article as soon as it is available.

You can find more information about Accepted Manuscripts in the [Information for Authors](#).

Please note that technical editing may introduce minor changes to the text and/or graphics, which may alter content. The journal's standard [Terms & Conditions](#) and the [Ethical guidelines](#) still apply. In no event shall the Royal Society of Chemistry be held responsible for any errors or omissions in this Accepted Manuscript or any consequences arising from the use of any information it contains.

Pyrolysis of sweet lemon (*Citrus limetta*) waste: Effect of zeolite β , ammonium on kinetics and bio-oil yield

Faisal Muhammad¹, Jan Nisar*¹, Ghulam Ali¹, Farooq Anwar*^{2,3}, Wan Azlina Wan Abdul Karim Ghani⁴, Ahsan Sharif⁵, Ejaz Ahmed⁵

¹*National Centre of Excellence in Physical Chemistry, University of Peshawar, Peshawar 25120, Pakistan*

²*Department of Food Science, Faculty of Food Science and Technology, Universiti Putra Malaysia, 43400 UPM Serdang, Selangor, Malaysia*

³*Institute of Chemistry, University of Sargodha, Sargodha-40100, Pakistan*

⁴*Sustainable Process Engineering Research Centre (SPERC), Department of Chemical and Environmental Engineering, Universiti Putra Malaysia, 43400 Serdang, Selangor, Malaysia*

⁵*School of Chemistry, University of the Punjab, New Campus, Lahore 54590, Pakistan*

Corresponding authors

(Jan Nisar): jan_nisar@uop.edu.pk or pashkalawati@gmail.com

(Farooq Anwar): farooq@upm.edu.my or fqanwar@yahoo.com



Abstract

This research aims to explore the potential of citrus waste for valuable products. A special pyrolysis chamber was used to produce bio-oil through thermo-catalytic pyrolysis of sweet lemon (*Citrus limetta*) waste using zeolite β , ammonium catalyst. Kinetic parameters were derived from thermogravimetric data using the Kissinger equation. The activation energy and frequency factor values for hemicellulose, cellulose, and lignin were determined to be 83.14, 108.08, and 124.71 kJ/mol, and 6.3×10^4 , 9.4×10^6 , 2.6×10^9 min⁻¹, respectively. GC-MS analysis of the bio-oil revealed a variety of fuel range hydrocarbons. Additionally, the biochar generated from non-catalytic and catalytic pyrolysis were compared which exhibited different surface characteristics as evident by Scanning Electron and Transmission Electron Microscopy depictions. Our findings indicated that the zeolite β , ammonium served as effective catalyst by reducing activation energy and lowering the temperature required for maximum degradation during pyrolysis, ultimately yielding a diverse array of useful products from citrus waste compared to non-catalyzed reaction. It was concluded from the fuel's properties that the bio-oil, if slightly upgraded using the appropriate techniques, had a promising future as a green fuel.

Keywords: Citrus wastes; Zeolite β , ammonium; Pyrolysis; Kinetics; Biochar; Bio-oil.



Nomenclature and Abbreviations

E _a	Activation energy
A	Frequency factor
β	Temperature programme rate
T _m	Temperature maximum degradation
R	Gas constant
GCMS	Gas chromatography mass spectrometry
FTIR	Fourier transforms infrared spectroscopy
TGA	Thermogravimetric analysis
SEM	Scanning electron microscopy
TEM	Transmission electron microscopy



1. Introduction

The rapid increase in population and shift in lifestyle have significantly heightened the demand for energy [1]. Fossil fuels have traditionally been the major source of energy [2], however, the industrialization and technology advancement have led to their accelerated consumption resulting in alarming depletion rates [3]. Furthermore, the combustion contributes to global warming, adversely affecting the environment [4]. In light of dwindling fossil fuels supplies and their potential role in climate change, researchers and the global community are actively seeking for environmentally friendly alternatives [5-7]. The urgent need to address fossil fuel shortages and their impact on climate change has become a global concern, prompting researchers and international organizations to explore sustainable energy sources. The United Nations Climate Panel has targeted 50 to 80% reduction in greenhouse gas emission by 2050, emphasizing the importance of switching to renewable energy sources from non-renewable ones. As a result, renewable energy is increasingly recognized as essential for sustainable development and environmental preservation [8].

Biofuels are gaining significant recognition as a green fuel due to their ability to emit fewer harmful gases, such as NO_x and SO_x, compared to fossil fuels. Recent years have seen a great deal of research being conducted on potential utilization of biomass to produce biofuels because of its affordable and environmentally sustainable nature [9, 10]. Biomass serves as promising source for mitigating harmful emissions, alongside other renewable sources [11, 12]. The utilization of biomass as a sustainable energy source is captivating due to its positive impact on the environment and eco-friendliness. One of the notable advantages of biomass conversion is its ability for compression into reduced volume, which facilitates easy storage, transportation, and long-term preservation without decomposition [13]. Moreover, the lifecycle analysis



indicates that biofuels, particularly biodiesel, can substantially reduce greenhouse gas (GHG) emissions as compared to petroleum diesel.

Citrus fruits are widely cultivated in many parts of the world and play a significant role in human nutrition [14]. Roughly half of the wet fruit mass is made up of citrus waste, which is produced by the fruit processing industry after juice is extracted. This waste primarily consists of peel and pulp [15]. Citrus peel and pulp, as a lignocellulosic material, predominantly consist of fibers and essential oils. These components can be extracted and utilized in various industries including medicinal and cosmetic. Moreover, the citrus fruit waste (peels and pulp), mainly consisted of hemicellulose, cellulose and lignin, can be utilized as a beneficial raw biomass for producing a variety of bio-chemicals and bio-fuels [16].

Worldwide, significant volumes of biomass waste are produced, including leftovers from the harvest and processing of fruit crops, which have significant potential to be transformed into biofuel. However, there is still a dearth of studies focusing on the pyrolysis kinetics of *Citrus limetta* waste over zeolite β , ammonium. Hence, the key objective of this work is to evaluate the efficacy of zeolite β , ammonium as catalyst for decomposition of citrus waste into biofuel. We also aim to appraise the kinetic parameters of reaction associated with this conversion. Additionally, we seek to find out how various parameters such as catalyst, temperature, and pyrolysis time affect the pyrolysis of *Citrus limetta* waste.

2. Experimental

2.1. Materials and Methods

The juice-extracted sweet lemon (*Citrus limetta*) waste (properly authenticated by a botanist), was sourced from a juice shop in Faisalabad city, Punjab, Pakistan. The collected biomass was shade-dried for 21 days, grinded into a fine powder using a grinder, sieved to the



desired mesh size, and stored in a sealed bag for further analyses. The elemental characteristics and structure of raw biomass were examined using energy dispersive X-rays and SEM. To improve the quality of oil produced, zeolite β , ammonium was selected as a catalyst among several commercial options.

2.2. Thermogravimetric Analysis of Citrus Waste and Kinetic Study

TGA of citrus waste loaded with zeolite β , ammonium was conducted on Q500 PerkinElmer at different temperature programme rate (15, 20, 25, and 30 °C.min⁻¹). The obtained TGA results were then used to determine the E_a and A-factor through the following Kissinger equation [17].

$$\ln\left[\frac{\beta}{T_m^2}\right] = \ln\left(\frac{A.R}{E_a}\right) - \frac{E_a}{RT_m} \quad (1)$$

In equation 1, T_m stands for maximum degradation temperature, β refers to temperature programme rate, and R denotes gas constant. The E_a and A-factor were computed from the slopes and intercepts of $\ln\beta/T_m^2$ vs $1000/T_m$ plots.

2.3. Pyrolysis Experiments and Products Characterization

In order to minimize heat loss in an inert atmosphere, citrus wastes loaded with zeolite β , ammonium catalyst was pyrolyzed in a salt bath (containing mixture of NaNO_2 , NaNO_3 and KNO_3) packed in a stainless-steel vessel enclosed in another vessel with insulating material. The pyrolysis process is schematically diagrammed in Figure 1 [18, 19]. For each experiment, 5 grams of citrus waste was placed in the reaction vessel and secured within the salt bath. The resulting vapours were directed through a condenser, where they were condensed into liquid fraction. A GC-MS machine (GC7890B MS5977B Agilent) was used to chemically characterize the recovered bio-oil. The analysis was carried out through HP-5 capillary column. Helium gas was employed as carrier gas and injector was kept in split mode at 25 °C. Column oven was



retained at 40 °C for 15 min and then increased to 160 °C at 10 °C.min⁻¹ and held for 8 min. After that, it was heated to 290 °C at a rate of 10 °C per minute and kept there for one minute. The analysis took a total of 24 minutes and the identities of peaks were made through NIST library. Moreover, the identity of the components in the bio-oil was also confirmed through FTIR analysis using Shimadzu IR Prestige-21.

The surface characteristics of biochar derived from both catalytic and non-catalytic processes were assessed employing SEM and TEM (JSM-5910 JEOL and JEM-2100 JEOL), respectively. For TEM investigation, the biochar was dissolved in acetone and then sonicated for five minutes. A drop of the sonicated colloidal solution was then placed onto a formvar-coated grid, allowed to air dry, and then transferred to the analytical chamber for examination.

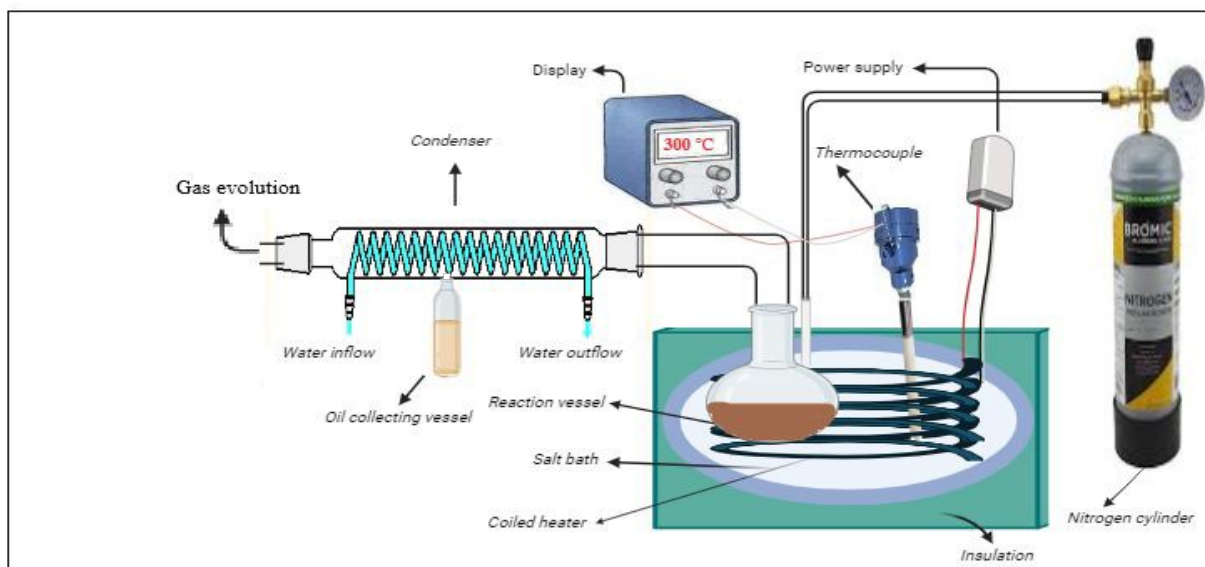


Figure 1. A schematic sketch of the pyrolysis setup

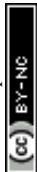


3. Results and Discussion

3.1 Raw Biomass Properties

The morphology and elemental analysis of raw *Citrus limetta* waste was studied using SEM-EDX. The SEM image is given in figure 2 which displays a highly porous structure. The disordered clusters with spongy holes are visible within the image. A thorough examination features closed-off microstructures, variable particle size distribution, and irregular and porous surfaces. The particles also varied in size and shape. The results are in conformity with some previous studies. Kamsonlian et al., [21] performed SEM analysis of orange peel and witnessed a porous surface with irregularly shaped pores of varying sizes. The surface morphology of lemon peel was also examined by Thirumavalavan et al., using SEM, and they found a porous surface with pore size of 39.483 Å.

Figure 3 represents the elemental composition of raw *Citrus limetta* waste having mass percentage of carbon (61.99%), oxygen (33.32%), potassium (3.23%) and calcium (1.46%) respectively. The results coincide with reported studies. Kamsonlian et al., [21] conducted EDX analysis of orange peel and observed the following weight percentages of chemical compositions: 33.22% C, 44.12% O, 13.02% K, 1.12% Si, 0.4% Ca, 1.30% Na, 1.34% Al, and 3.30%Mg. According to Palaniappan et al.'s EDX study of sweet orange (*Citrus x sinensis*) fruit waste, carbon and oxygen were the largest in the sample, which include 35.5 and 42.6%, respectively.



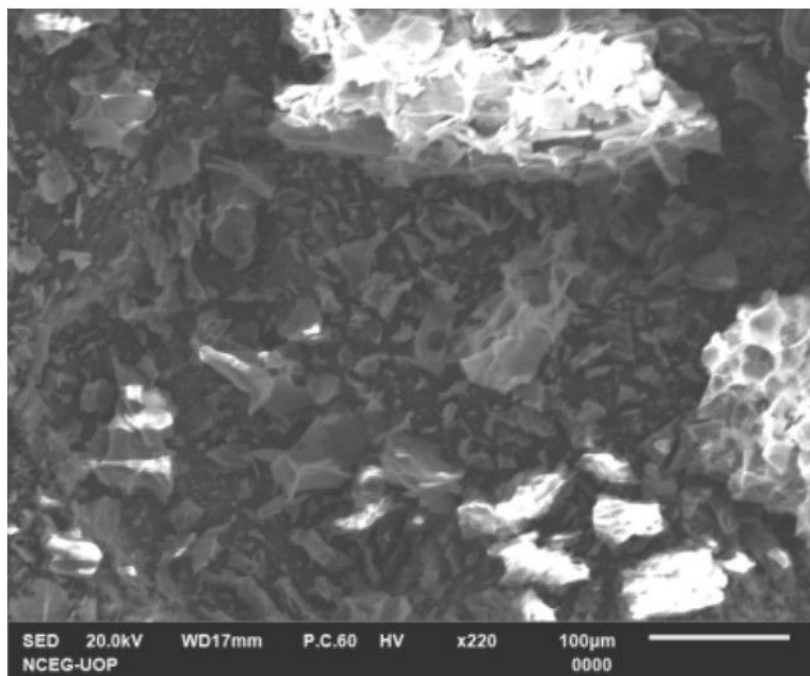


Figure 2. SEM depiction of *Citrus limetta* waste

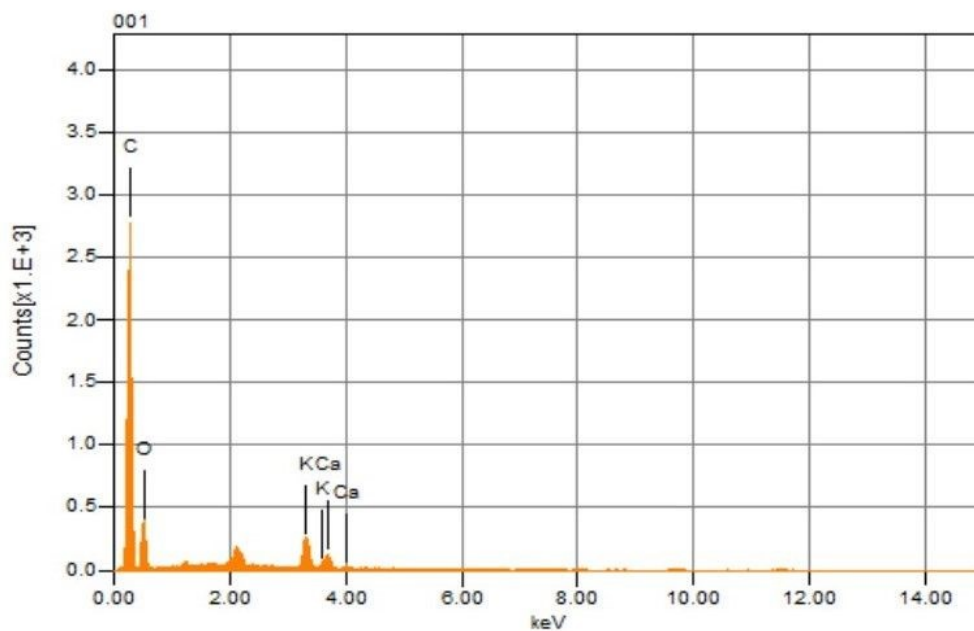
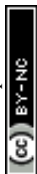


Figure 3. EDX of *Citrus limetta* waste



3.2. Thermogravimetric analysis and Kinetics

Thermogravimetry of citrus waste loaded with zeolite β , ammonium was conducted at a temperature programme rate of $15\text{ }^{\circ}\text{C}\cdot\text{min}^{-1}$, and the results are portrayed in TG/DTG curve shown in figure 4 and table 1 [24]. Utilizing the curve deconvolution method and application of Lorentzian peak function to TG curve, it was determined that weight loss occurred in four distinct phases between room temperature and 600°C , with no additional peak was noted. The initial weight loss was attributed by the physical desorption of vapours at temperature below $100\text{ }^{\circ}\text{C}$. For hemicellulose, the T_{max} was determined to be $223\text{ }^{\circ}\text{C}$. In the case of cellulose degradation, the T_{max} was found to be $318\text{ }^{\circ}\text{C}$, while for lignin, it was observed at $436\text{ }^{\circ}\text{C}$. These findings align with earlier investigations. Nisar et al., [25] studied the pyrolysis of sugarcane bagasse with and without CuO. Their findings revealed a consistent four-step weight loss processes, which was attributed by the elimination of moisture and the breakdown of hemicelluloses, cellulose, and lignin. Additionally, Azariah et al., [26] performed banana peel pyrolysis at $10^{\circ}\text{C}/\text{min}$ up to $800\text{ }^{\circ}\text{C}$, they observed 5.2% weight loss from 145 to 240°C , 45.9% weight loss from 240 to $448\text{ }^{\circ}\text{C}$, while 26.4% weight loss from 448 to $800\text{ }^{\circ}\text{C}$.



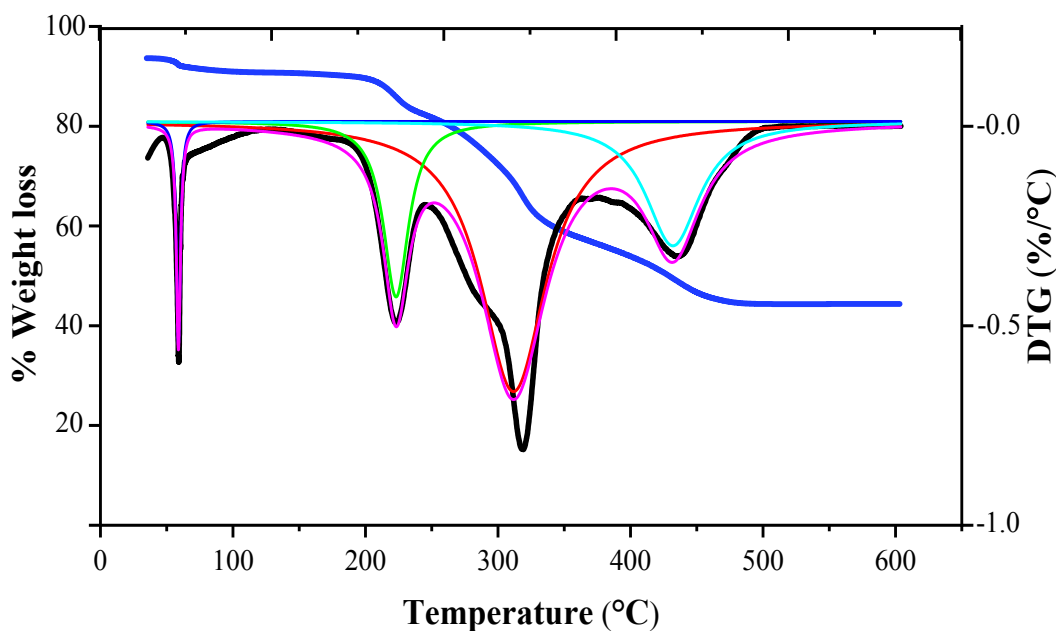


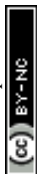
Figure 4. TG/DTG of *Citrus limetta* waste in the presence of zeolite β , ammonium at heating rate of $15\text{ }^{\circ}\text{C}\cdot\text{min}^{-1}$

Table 1. Data obtained from TG/DTG of *Citrus limetta* waste in the presence of zeolite β , ammonium at $15\text{ }^{\circ}\text{C}\cdot\text{min}^{-1}$

Temp/ $^{\circ}\text{C}$	$T_{\text{max}}/^{\circ}\text{C}$	Component
179 – 280	223	Hemicellulose
280 – 391	318	Cellulose
391 – 527	436	Lignin



For the kinetic study thermal degradation experiments of citrus waste loaded with zeolite β , ammonium were conducted at temperature programme rate of 15, 20, 25, 30 °C·min⁻¹. The obtained data were used to determine E_a and A-factor applying Kissinger equation. The plots of $\ln\beta/T_m^2$ vs $1000/T_m$ were constructed (figure 5), allowing for the extraction of E_a and A-factor from the resulting graphs. The calculated values (table 2) showed that zeolite β , ammonium acted as good catalyst for citrus waste decomposition, evidenced by lower activation energies required for the decomposition of hemicellulose (83.14 kJ·mol⁻¹), cellulose (108.08 kJ·mol⁻¹) and lignin (124.71 kJ·mol⁻¹) compared to non-catalytic reactions, which showed activation energies of 99.76, 157.96, and 174.59 kJ·mol⁻¹, respectively [27]. This trend aligns with findings from other biomass pyrolysis studies. For example, in a study on decomposition of peanut shells the authors, calculated E_a values (by Kissinger method) in the absence of catalyst as 108.1, 116.4, and 182.9 kJ·mol⁻¹ for hemi-cellulose, cellulose, and lignin, respectively. However, in the presence of catalyst, the E_a values were found as 66.5, 74.8, and 133 kJ·mol⁻¹ for the same components, exhibiting termite hill as an efficient catalyst [28]. Varma et al., [29] used a thermogravimetric analyzer to conduct pyrolysis studies of peanut shells at heating rate of 10, 20, and 30 °Cmin⁻¹. The Kissinger equation was used to determine E_a and A-factor. The calculated average E_a was observed as 109.05 kJ/mol. Similarly, in a study on sugarcane bagasse decomposition using Kissinger method [30], a reduction in E_a values were noted for catalyzed decomposition of hemicellulose, cellulose, and lignin vis-a-vis un-catalyzed reaction. Velazquez et al., [31] conducted pyrolysis of orange waste and calculated activation energies as 117, 105 and 260 kJ/mol for decomposition of hemicellulose, cellulose and lignin, respectively.



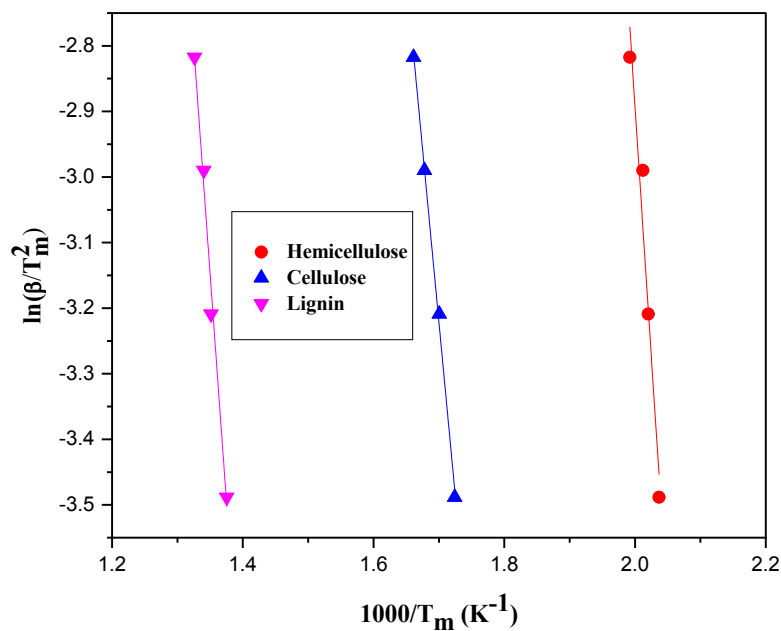


Figure 5. Kissinger plots constructed from degradation of *Citrus limetta* waste loaded with zeolite β , ammonium

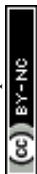
Table 2. Kinetic parameters calculated employing Kissinger method

Component	Parameters		
	Ea/kJ·mol ⁻¹	A/min ⁻¹	R ²
Hemicellulose	83.14	6.3×10 ⁴	0.979
Cellulose	108.082	9.4×10 ⁶	0.939
Lignin	124.71	2.6×10 ⁹	0.951



3.3 Optimization of experimental conditions for pyrolysis

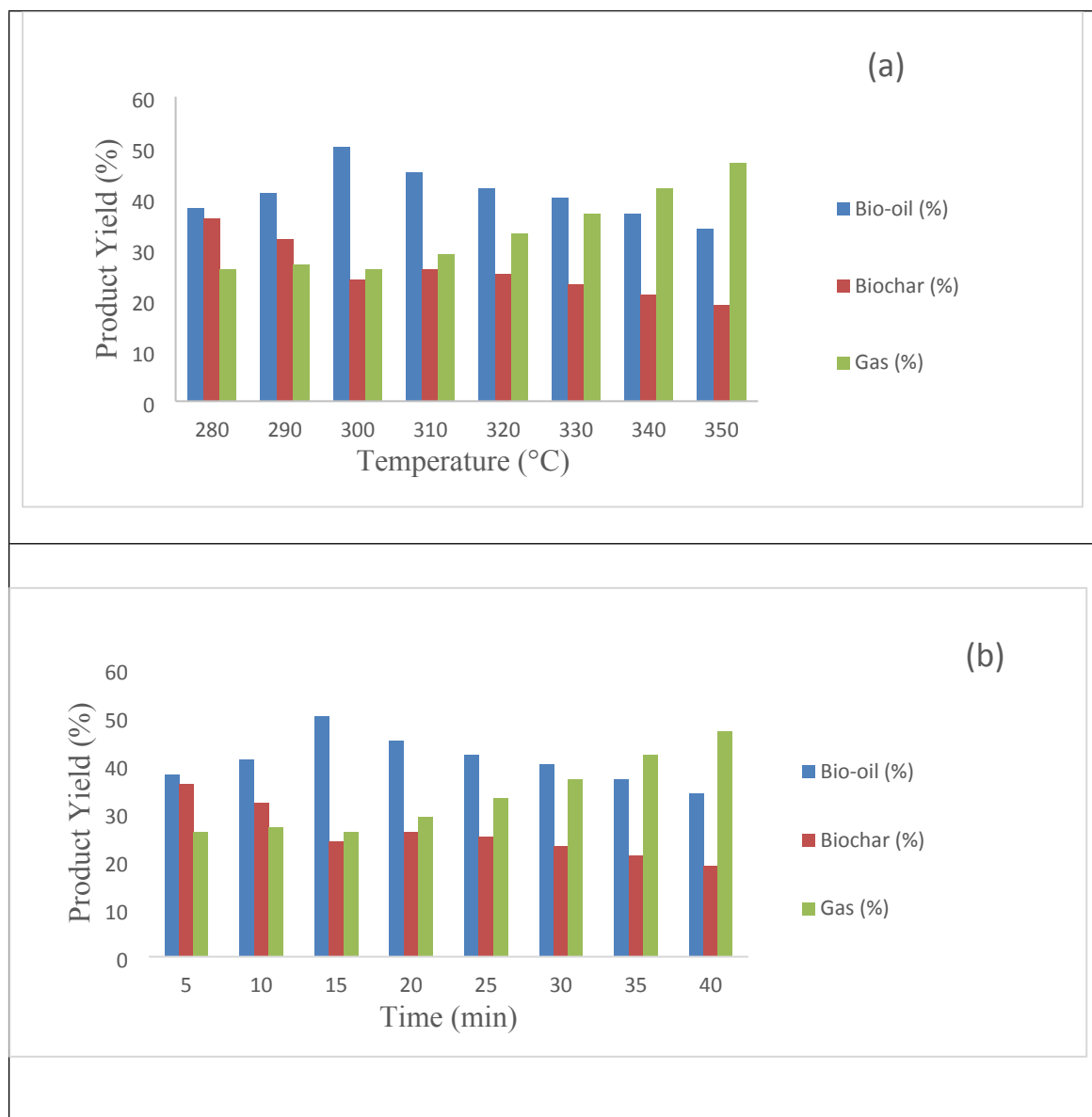
Pyrolysis tests were carried out between 280 and 350 °C to evaluate how temperature affects the pyrolysis of citrus waste. The pyrolysis products from citrus wastes treated with zeolite β , ammonium at varying temperatures, catalyst concentrations and reaction times are shown in figures 6a, 6b and 6c, respectively. These figures depict the resulting bio-oil, char and gas yields, highlighting the influence of experimental conditions on the distribution of pyrolysates. Figure 6a illustrates the effect of temperature on the catalytic degradation of citrus waste. The plot indicates that the production of liquid product increased gradually, peaking at 300 °C before declining with further increase in temperature. In contrast, the yield of gas fraction improved steadily as temperature rose. These results demonstrate that the use of zeolite β , ammonium catalyst effectively lowered the temperature required for maximum bio-oil production from citrus waste, establishing 300 °C as the optimal temperature for oil production with this catalyst. This suggests that zeolite β , ammonium outperform pumice, as reported in our previous investigation [27]. For comparison, Zhang et al., [32] examined that the optimum temperature for hydrothermal liquefaction of lemon peel was 336°C, which is very close to our data. Additionally, Alvarez et al., [33] achieved a 54.6% (by weight) yield of bio-oil at 425°C during the fast pyrolysis of citrus waste. Moreover, the figure demonstrates that as the temperature increases, the gaseous fraction rises while the bio-oil shrinkages, which is attributed to the secondary degradation of bio-oil [34]. Miranda et al., [35] conducted bench-scale pyrolysis experiments of citrus waste and observed that increasing pyrolysis temperature resulted in decreased char yield while increasing volatile content. Another primary objective of this work is to find out the optimal time at optimum temperature for pyrolyzing citrus waste. Figure 6b illustrates the time optimization of the pyrolysis reaction. The maximum oil was produced at



time of 15 minutes, beyond which the production of bio-oil decreased. It also indicates that an increase in residence time led to a higher gaseous yield, while the biochar yield decreased with prolonged time. These findings align closely with a previous study on the degradation of sesame biomass [36].

To determine the impact of zeolite β , ammonium concentration on the pyrolysates yield, the sample was mixed with varying percentages of zeolite β , ammonium (1%, 3%, 5%, 7%, and 9%) at optimal temperature and time. The results are given in figure 6c. When catalyst was combined with the sample up to 5%, maximum bio-oil was obtained. Beyond that concentration it has a negative effect. This is because raising the concentration of the catalyst causes the liquefaction to grow, but it also has an adverse effect above the ideal threshold of 5%. Additionally, catalyst poisoning is caused by the bio-oil molecules' adsorption of the catalysts' high specific surface area. This trend is in line with several previous works. Samolada et al., [37] studied pyrolysis of lignocellulose and discovered that enhancing the zeolite content lowered the amount of bio-oil while increasing the amount of gases. Through pyrolysis of citrus waste, Poddar et al., [38] showed that the action of ZnO enhanced the bio-oil output (49.39 wt.%) as compared to non-catalytic ones (30.75 wt.%). Furthermore, gas production was found to increase with rise in temperature.





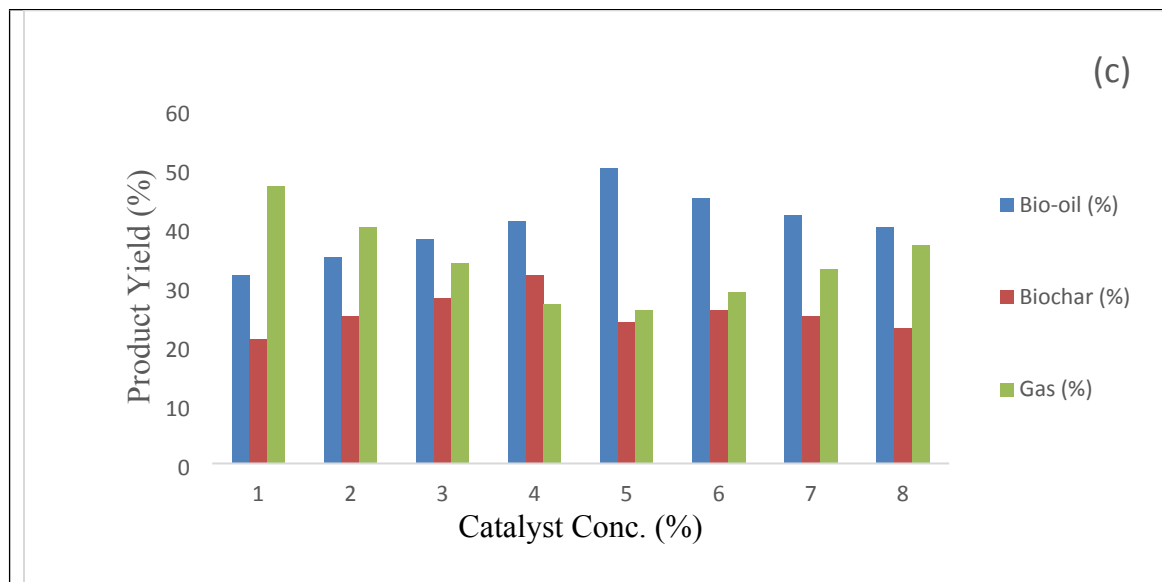


Figure 6. Pyrolysis of *Citrus limetta* loaded with zeolite β , ammonium (a) Temperature optimization (b) Time optimization (c) Catalyst optimization



A comparison of oil yield in this work with previous studies is presented in table 3. It is clear from the data that sufficient quantity of bio-oil (50%) was produced from *Citrus limetta* waste in the existence of zeolite β , ammonium at lower temperature of 300 °C.

Table 3. Pyrolysates yield from different biomasses at various conditions.

Biomass	Catalyst	Optimum Temp./°C	Product yield/wt. %			Reference
			Bio-oil	Gases	Bio-char	
Grapefruit waste	Nickel oxide	420	33	35	32	[19]
Almond shells	Zinc oxide	420	40	10	50	[18]
Cotton seed press cake	Nickel doped zeolite Y, hydrogen	300	35	17	48	[39]
Pomegranate peels	Sulfonated tea waste	330	56	6	37	[9]
<i>Citrus limetta</i> waste	Pumice	320	45	20	35	[7]
<i>Citrus limetta</i> waste	Zeolite β , ammonium	300	50	26	24	This work



3.4 Characterization of Pyrolysates

3.4.1 GC-MS Analysis of Bio-oil

A GC-MS machine was employed to chemically characterize the produced bio-oil and the chromatogram is depicted in figure 7. A detailed summary of the identified products, including their molecular formula, name, molecular weight, percent area, and retention time, is provided in Table 4. The current findings indicate that catalytic pyrolysis greatly enhanced both quantity and diversity of oil components produced compared to our previous study [28]. Notably, when comparing the catalytic bio-oil derived from citrus waste with the non-catalytic bio-oil [27], it was noted that the bio-oil produced with zeolite β , ammonium contained certain fuel range components, such as phenol and benzene derivatives. Additionally, the analysis revealed the presence of a variety of compounds like furan, maltol, creosol, ester and oleic acid, suggesting that the bio-oil has been upgraded and could serve as promising candidate for biofuel. The results imply that zeolite β , ammonium played a crucial role in improving bio-oil quality by increasing the variety of compounds detected by GC/MS and expanding the spectrum of hydrocarbons present.

The results align with previous investigations in the field of catalytic pyrolysis. Bhoi et al., [40] explored the catalytic pyrolysis of biomass using zeolite-based catalysts designed to eliminate undesirable compounds and enhance the hydrocarbon yield in bio-oil. Similarly, Miranda et al., [35] utilized GC/MS to identify key components such as carboxylic acid, phenol, and aldehyde in the the bio-oil produced by quickly pyrolyzing citrus dry peel. Significant compounds discovered were benzene, phenol, n-hexadecenoic acid, and 2-cyclopenten-1-one, 2-methyl. In another study, Qiao et al., [41] reported the presence of terpenic oxide, alcohols, esters, ketone, and aldehydes in the liquid fraction obtained from citrus peels. Additionally, Kravetz et al., [42] discovered large peaks of 2-propanone, 1-hydroxy, 2-propenoic acid,



succindialdehyde, furfural, 2-furanmethanol, 2(5H)-furanmethanol, and 3-methyl, 4-methyl-5H-furan-2-one in in the bio-oil from *Citrus sinensis* waste.

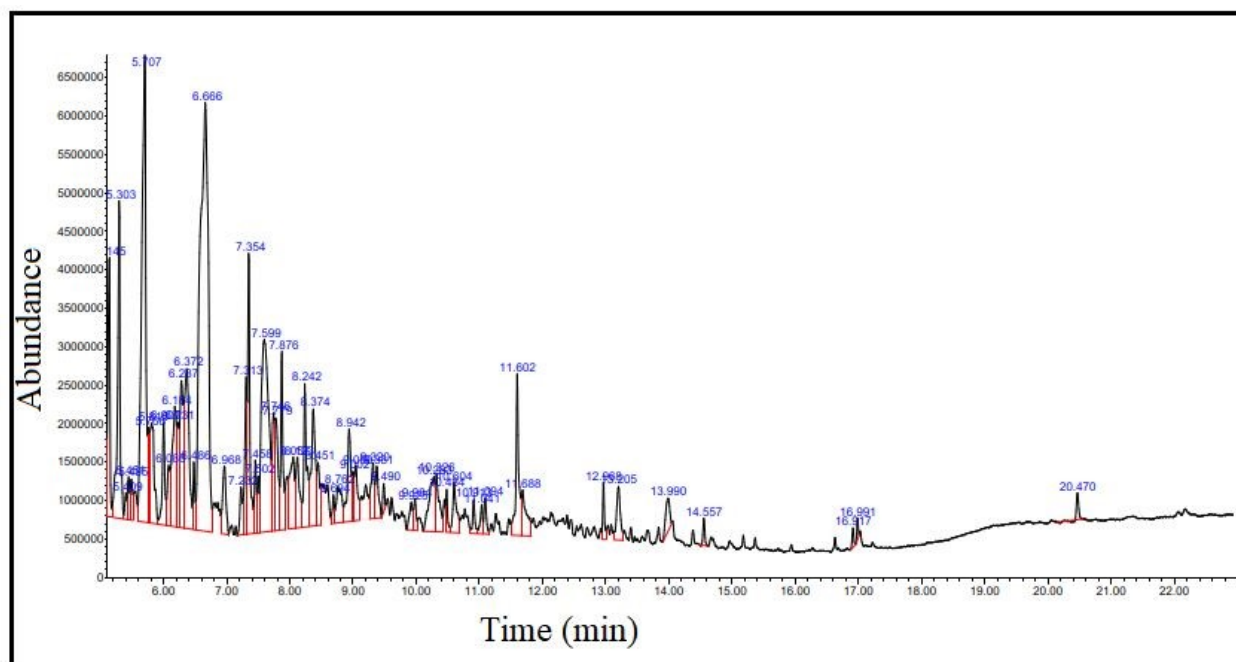


Figure 7. GC-MS chromatogram of bio-oil produced by thermo-catalytic decomposition of *Citrus limetta* waste

Table 4. GC-MS profiling of chemical compounds in bio-oil produced by thermo-catalytic decomposition of *Citrus limetta* waste

S.No.	R/T(min)	Component	Chem. formula	Mol. Wt	Area %
1	5.14	Maltol	$C_6H_6O_3$	126.11	2.81
2	5.30	Hydrazine, 3 fluorophenyl	$C_6H_7FN_2$	126.13	4.18
3	5.41	Triethylenediamine	$C_6H_{12}N_2$	112.17	0.23
4	5.45	Furan, 4-methyl-2-propyl	$C_8H_{12}O$	124.18	0.44
5	5.49	2(1H)-Pyridinone	C_5H_5NO	95.09	0.49
6	5.71	4H-Pyran-4-one,2,3-dihydro-3,5-dihydroxy-6-methyl	$C_6H_8O_4$	144.12	9.68
7	5.77	4(1H)-Pyridone	C_5H_5NO	95.09	0.79
8	5.81	3-Pyridinol	C_5H_5NO	95.09	2.24
9	6.01	Phenol, 3-amino	C_6H_7NO	109.12	1.36
10	6.09	2(3H)-Furanone, dihydro-5-pentyl	$C_9H_{16}O$	156.22	0.79
11	6.18	2(3H)-Furanone, 5-butylidihydro	$C_8H_{14}O_2$	142.19	2.72
12	6.23	2-Hydroxy-5,5-dimethyl-hex-2-en-4-one	$C_8H_{14}O_2$	142.20	1.04
13	6.29	Furan, 2-ethoxy-2,3-dihydro-4-methyl	$C_7H_{12}O_2$	128.17	2.41



14	6.37	2-Pentene, 1-(pentyloxy)-, (E)-(E)-1-Pentyloxy-2-pentene	C ₁₀ H ₂₀ O	156.26	4.05
15	6.49	2-Hydroxy-3-propyl-2-cyclopenten-1-one	C ₈ H ₁₂ O ₂	140.17	0.62
16	6.67	Phenol, 2-ethoxy	C ₈ H ₁₀ O ₂	138.16	17.79
17	6.97	2,5-Dimethyl-4-hydroxy-3(2H)-furanone	C ₆ H ₈ O ₃	128.13	1.21
18	7.23	meta-Methoxybenzenethiol	C ₇ H ₈ OS	140.20	0.57
19	7.31	1,2-Benzenediol,3-methyl	C ₇ H ₈ O	124.13	1.68
20	7.35	1,4-Benzenediol, 2,3,5-trimethyl	C ₉ H ₁₂ O ₂	152.19	3.30
21	7.46	Phenol, 4-ethyl-2-methoxy-	C ₉ H ₁₂ O	152.19	0.74
22	7.50	Creosol	C ₈ H ₁₀ O ₂	138.16	0.50
23	7.59	6-Methyl-3(2H)-pyridazinone	C ₅ H ₆ N ₂ O	110.11	7.32
24	7.75	Benzoic acid, 2,3-dihydroxy	C ₇ H ₆ O ₄	154.12	1.43
25	7.78	1,2-Benzenediol, 4-methyl	C ₇ H ₈ O	124.13	1.87
26	7.88	2-Methoxy-4-vinylphenol	C ₉ H ₁₀ O ₂	150.22	1.95
27	8.06	2,5-Diethylphenol	C ₁₀ H ₁₄ O	150.22	1.79
28	8.12	3-Thiophenecarboxylic acid	C ₅ H ₄ O ₂ S	128.15	1.44
29	8.24	Phenol, 2,6-dimethoxy-	C ₈ H ₁₀ O ₃	154.16	2.11
30	8.37	1,4-Benzenediol, 2-methyl-	C ₇ H ₈ O ₂	124.13	2.54
31	8.45	2-Ethyl-4,6-dimethyltetrahydropyran	C ₉ H ₁₈ O	142.24	0.78
32	8.69	2,5-Dihydroxypropiophenone	C ₉ H ₁₀ O ₃	166.17	0.30
33	8.76	3-Cyclohexen-1-one,2-isopropyl-5-methyl	C ₁₀ H ₁₆ O	152.23	0.99
34	8.94	Benzene, 2-fluoro-1,3,5-trimethyl-	C ₉ H ₁₁ F	138.18	1.65
35	9.01	Acetic acid, heptyl ester	C ₉ H ₁₈ O ₂	158.23	0.52
36	9.05	4-Hydroxy-5,6-epoxy-.beta.-ionone	C ₁₃ H ₂₀ O ₃	224.30	0.91
38	9.38	Phenol, 2-methoxy-3-methyl ester	C ₈ H ₁₀ O ₂	138.16	0.82
39	9.49	2,4,6-Octatriene, 2,6-dimethyl-	C ₁₀ H ₁₆	136.23	0.24
40	9.92	Benzene, 4-ethyl-1,2-dimethoxy	C ₁₀ H ₁₄ O ₂	166.21	0.43
41	9.98	Tricyclo[3.3.2.0(3,7)]decan-9-one	C ₁₀ H ₁₄ O	150.22	0.42
42	10.28	1,3-Oxathiolane,2-(4 chlorophenyl)-2-methyl	C ₁₀ H ₁₁ ClOS	214.71	1.62
43	10.33	3-Hydroxy-4-methoxybenzoic acid, methyl ester	C ₉ H ₁₀ O ₄	182.17	1.12
44	10.48	5-tert-Butylpyrogallol	C ₁₀ H ₁₄ O ₃	182.22	0.41
45	10.60	Cyclopropane,1-ethoxy-2,2-dimethyl-3-(2 phenylethenylidene)	C ₁₅ H ₁₈ O	214.31	0.97
46	10.91	3H-Benz[e]indene, 2-methyl	C ₁₄ H ₁₂	180.24	0.41
47	11.04	Anthracene, tetradecahydro	C ₁₄ H ₂₄	192.34	0.35
48	11.09	Carbamic acid, methylphenyl-, ethyl ester	C ₁₀ H ₁₃ NO ₂	179.22	0.45
49	11.60	3,4-Dichlorobenzenethiol	C ₆ H ₃ SHCl ₂	179.07	2.33
50	11.69	Hydrazine, (2,4-dichlorophenyl)	C ₆ H ₆ C ₁₂ N ₂	177.03	1.16
51	12.97	Ethyl,4-hydroxy-3-methoxyphenylacetate	C ₁₁ H ₁₄ O ₄	210.23	0.51
52	13.20	2,4-Imidazolidinedione,5-(4-hydroxyphenyl)	C ₉ H ₈ N ₂ O ₃	192.17	1.06
53	13.99	beta.-(4-Hydroxy-3-methoxyphenyl)propionic acid	C ₁₀ H ₁₂ O ₄	196.19	0.69
54	14.56	5,10-Diethoxy-2,3,7,8-tetrahydro-1H,6H-dipyrrolo[1,2-a:1',2'd] pyrazine	C ₁₄ H ₂₂ N ₂ O ₂	250.34	0.25
55	16.92	9,12-Octadecadienoic acid (Z,Z)	C ₁₈ H ₃₂ O ₂	280.44	0.16
56	16.99	6-Octadecenoic acid	C ₁₈ H ₃₄ O ₂	282.50	0.14
57	20.47	Dicyclohexyl phthalate	C ₂₀ H ₂₆ O ₄	330.40	0.26



3.4.2 FTIR of Bio-oil

Figure 8 shows FTIR spectrum of bio-oil. For the alcohols and phenols that make up major components of citrus peels, a strong peak (at 3448 cm^{-1}) is indicative of OH bond stretching, while a weak peak (at 1384 cm^{-1}) is due to OH bending. The C=C stretch can be seen by the peak at 2067 cm^{-1} . The C=O stretching of ketones, carboxylic acids, and esters is indicated by the absorbance peak at 1713 cm^{-1} and 1637 cm^{-1} . The peak at 1268 cm^{-1} due to C-O stretching vibrations is pointing towards the existence of carboxylic acids, ethers, alcohols and esters. Aliphatic amines are indicated by the C-N stretching vibrations at 1050 cm^{-1} . These outcomes from FTIR are in conformity with the study of Al-Layla et al., [43] on pyrolysis of milk thistle waste.

In another study, lemon grass was flash-pyrolyzed by Madhu et al. [44] and FTIR was used to examine the produced bio-oil. The primary functional groups recognized were associated with C=O stretching (carbonyls), C-O stretching (alcohols, ethers, carboxylic acids, and esters), C-N stretching (aliphatic amines) and OH (alcoholic and phenols). Likewise, Volpe et al. [45] utilized leftover orange and lemon peels to produce bio-oil. The functional groups they examined, according to FTIR analysis, were OH stretching (phenol), C=O stretching (ketone and carboxylic acids), and OH bending at 1370 cm^{-1} .



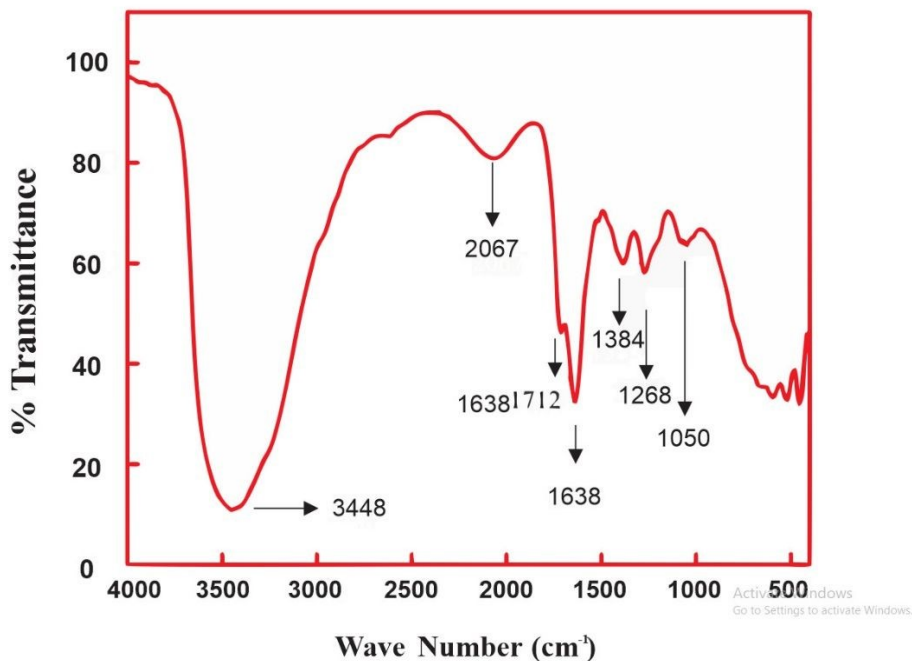


Figure 8. FTIR spectrum of pyrolysis oil extracted from *Citrus limetta* waste

3.4.3 Fuel Properties of the Bio-oil

As indicated by the physico-chemical characteristics, the bio-oil produced has a strong odor and was pale yellow in color. Other characteristics (Table 5) of the tested bio-oil, including, density, viscosity and pH, were quite similar to those of bio-oils testified in previous research [46, 47].



Table 5. Comparison of physico-chemical properties of bio-oil obtained from *Citrus limetta* waste with bio-oil from different sources

Biomass/catalyst	Density (kgm ⁻³)	Viscosity (Pa.s)	pH	Reference
Rice husk	1190	0.150	2.80	[48]
Pine wood (at 425 °C)	1174 ± 40	-	2.1 ± 0.09	[49]
Miscanthus	1050	-	2.95	[50]
Corn stover	1250	-	2.87	
Wood pellets	1230	-	2.80	
Cotton stalk	1160	0.140	-	[51]
Areca nut husk	980	0.078	-	[46]
Areca nut husk/ ZSM-5	812	0.029	-	[46]
Cow hooves	1030±100	0.010	-	[52]
Sugarcane bagasse	1211	0.004	-	[53]
Palm shell	1051	0.003	-	[54]
Pinewood waste	1140	0.001	-	[55]
Corn stalk	1220	0.168	3.20	[47]
Sweet lemon waste (at 300 °C)	980	0.168	3.5	This work



3.4.4 Characterization of Biochar

Figure 9a and 9b display the SEM images of non-catalytic and catalytic biochar, respectively. The biochar obtained from non-catalytic decomposition (figure 9a) reveals a smooth disc-like texture, while catalytic biochar (figure 9b) exhibits an uneven and rough surface which makes it suitable for many applications for example as adsorbent, energy storage super capacitor, and catalyst [56]. These characteristics in biochar can be achieved through pyrolysis of citrus wastes using a selected catalyst. The interaction between the catalyst and citrus wastes resulted in the formation of lumps-like structures in catalytic biochar, which possessed a larger surface area. The use of a catalyst induced significant morphological changes, causing surface deformation with highly developed pore structure as also observed by many authors. Wang et al., [57] studied biochar produced after pyrolysis and observed irregular distributed pores on its surface that have been broken and collapsed. Ali et al., [20] performed SEM analysis on both non-catalytic and catalytic biochar samples. They observed flat and disc-like surface of non-catalyzed biochar as compared to catalytic biochar having uneven, irregular and porous structure.



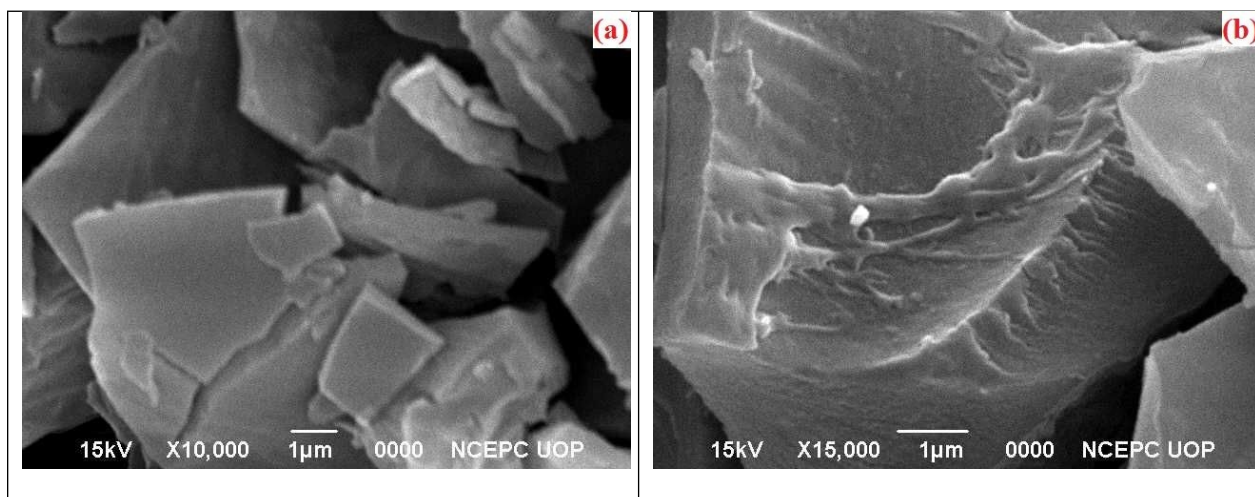
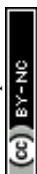


Figure 9. SEM images of *Citrus limetta* waste biochar (a) without zeolite β , ammonium (b) with zeolite β , ammonium

Transmission Electron Microscopy was employed to study the microstructure of *Citrus limetta* waste biochar. Figure 10 (a, b and c) presents the TEM images of non-catalytic biochar. The TEM images of the non-catalytic biochar revealed a fused carbon skeleton, resulting in a compact structure with small, rigid and even surface. In contrast, the biochar obtained from catalytic process exhibited a different morphology as exhibited in figure 10 (d, e and f). The TEM images show increase in the surface pore size, resulting from the agglomeration of carbon particles. This agglomeration process captured carbon molecules, imparting various rubber-like qualities to the biochar. The acquired data is in agreement with the findings reported in existing literature. Ali et al., [20] performed TEM analysis of both un-catalyzed and catalyzed biochar samples. They observed that the bare biochar exhibited a small particle size and displayed a highly rigid structure. In contrast, the catalytic biochar showed irregular surface and large pore size produced as a result of agglomeration of carbon particles. Li et al., [58] carried out TEM



analysis of biochar and revealed accumulation of similar carbon particles which were equally distributed in the carbon matrix.

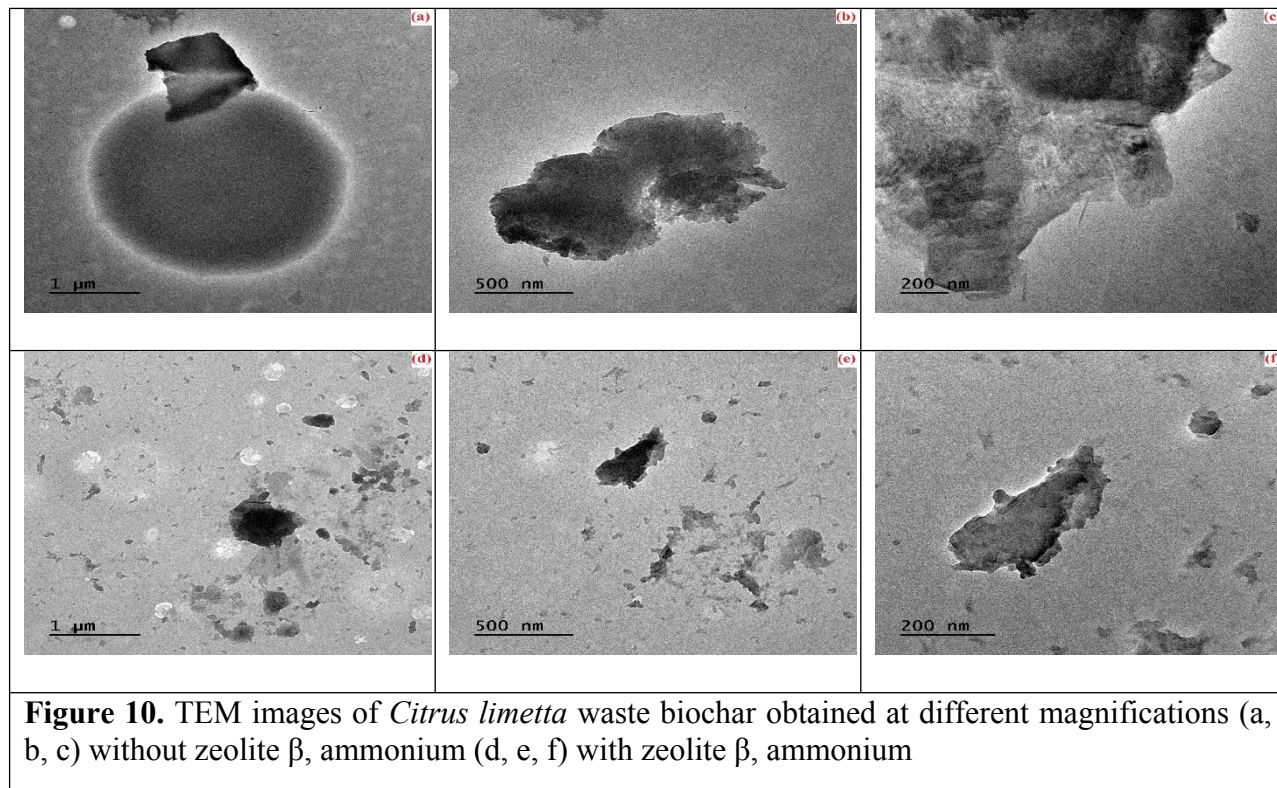


Figure 10. TEM images of *Citrus limetta* waste biochar obtained at different magnifications (a, b, c) without zeolite β , ammonium (d, e, f) with zeolite β , ammonium



4. Conclusions

Our research centered on utilizing zeolite β , ammonium as catalyst for pyrolysis to transform waste citrus materials into valuable products, while also figuring out the reaction's kinetic parameters. Thermogravimetric analysis was conducted on citrus waste in an inert atmosphere over zeolite β , ammonium at various heating rates. Using Kissinger method, E_a for hemicelluloses, cellulose, and lignin was determined as 83.14, 108.082, and 124.71 kJ/mol, respectively. Moreover, for bio-oil production pyrolysis was done in a particular salt bath in nitrogen environment at 280 - 350 °C in the presence of zeolite β , ammonium catalyst. The pyrolyzed oil obtained at the optimized conditions was characterized using GC-MS and it was found that some additional fuel range hydrocarbons were noticed as compared to non-catalyzed reaction. The existence of phenols and alcohols, the primary constituents of citrus peel, was further verified by FTIR spectrum data. Furthermore, additional bending oriented and stretching-supporting peaks verified the occurrence of carboxylic, ether, alcoholic, esters, and aliphatic amine groups. In general, the findings of this investigation indicated that the use of zeolite β , ammonium not only improved the quality of oil but also reduced the temperature and E_a of pyrolysis reaction. The work reported herein reveals that citrus waste in presence of zeolite β , ammonium catalyst has enormous potential for use in the production of biofuel. It can also be argued that, with the appropriate upgrading, the oil produced by citrus waste could be utilized as alternative biofuel.



Authors' contributions

Faisal Muhammad., Investigation, Methodology, Writing - original draft. Jan Nisar., Conceptualization, Funding acquisition, Resources, Project administration. Ghulam Ali., Writing, Results and analysis. Farooq Anwar., Review and editing. Wan Azlina Wan Abdul Karim Ghani., Review and editing and visualization. Ahsan Sharif., Editing and visualization. Ejaz Ahmed., Editing and visualization

Competing interests

The authors have no conflicts of interest to declare

Acknowledgements

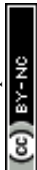
Higher Education Commission, Pakistan is acknowledged for Grant No. 20-1491.

REFERENCES

1. Avtar, R., et al., *Population–urbanization–energy nexus: a review*. Resources, 2019. **8**(3): p. 136.
2. Akram, F., et al., *Current trends in biodiesel production technologies and future progressions: A possible displacement of the petro-diesel*. Journal of Cleaner Production, 2022: p. 133479.
3. Al Rashdan, M., M. Al Zubi, and M. Al Okour, *Effect of using new technology vehicles on the World's environment and petroleum resources*. Journal of Ecological Engineering, 2019. **20**(1).
4. Afraz, M., et al., *Production of value added products from biomass waste by pyrolysis: An updated review*. Waste Management Bulletin, 2024. **1**(4): p. 30-40.
5. Nisar, J., et al., *Production of Bio-Oil from De-Oiled Karanja (Pongamia pinnata L.) Seed Press Cake Via Pyrolysis: Kinetics and Evaluation of Anthill as the Catalyst*. Sustainable Chemistry, 2022. **3**(3): p. 345-359.
6. Waqas Ahmad, J.N., Farooq Anwar, Faisal Muhammad, *Future prospects of biomass waste as renewable source of energy in Pakistan: A mini review*. Bioresource Technology Reports, 2023: p. 101658.
7. Muhammad, F., et al., *Improved bio-oil yield from thermo-catalytic pyrolysis of Citrus limetta waste over pumice: Determination of kinetic parameters using Kissinger method*. Bioresource Technology Reports, 2023. **24**: p. 101635.
8. Amin, M., et al., *Hydrogen production through renewable and non-renewable energy processes and their impact on climate change*. International journal of hydrogen energy, 2022. **47**(77): p. 33112-33134.
9. Rehman, N.U., et al., *Production of bio-oil from thermo-catalytic decomposition of pomegranate peels over a sulfonated tea waste heterogeneous catalyst: a kinetic investigation*. Energies, 2023. **16**(4): p. 1908.
10. Nisar, J., et al., *Thermo-catalytic decomposition of walnut shells waste over cobalt doped cerium oxide: Impact of catalyst on kinetic parameters and composition of bio-oil*. Chemical Engineering Science, 2023. **282**: p. 119355.



11. Ahmed, S.F., et al., *Utilization of nanomaterials in accelerating the production process of sustainable biofuels*. Sustainable Energy Technologies and Assessments, 2023. **55**: p. 102894.
12. Choudhary, S., et al., *Pulses Waste to Biofuels, in Agroindustrial Waste for Green Fuel Application*. 2023, Springer. p. 1-26.
13. Miao, W., et al., *Biochar application enhanced rice biomass production and lodging resistance via promoting co-deposition of silica with hemicellulose and lignin*. Science of The Total Environment, 2023. **855**: p. 158818.
14. Liu, Y., E. Heying, and S.A. Tanumihardjo, *History, global distribution, and nutritional importance of citrus fruits*. Comprehensive reviews in Food Science and Food safety, 2012. **11**(6): p. 530-545.
15. Kundu, D., et al., *Citrus fruits, in Valorization of Fruit Processing By-products*. 2020, Elsevier. p. 145-166.
16. Selvarajoo, A., et al., *Biochar production via pyrolysis of citrus peel fruit waste as a potential usage as solid biofuel*. Chemosphere, 2022: p. 133671.
17. Blaine, R.L. and H.E. Kissinger, *Homer Kissinger and the Kissinger equation*. Thermochemica acta, 2012. **540**: p. 1-6.
18. Nisar, J., et al., *Pyrolysis of almond shells waste: effect of zinc oxide on kinetics and product distribution*. Biomass Conversion and Biorefinery, 2022. **12**(7): p. 2583-2595.
19. Nisar, J., et al., *Pyrolysis of juice-squeezed grapefruit waste: Effect of nickel oxide on kinetics and bio-oil yield*. International Journal of Environmental Science and Technology, 2022. **19**(10): p. 10211-10222.
20. Ali, G., et al., *Production of Fuel Range Hydrocarbons from Pyrolysis of Lignin over Zeolite Y, Hydrogen*. Energies, 2023. **16**(1): p. 215.
21. Kamsonlian, S., et al., *Characterization of banana and orange peels: biosorption mechanism*. International Journal of Science Technology & Management, 2011. **2**(4): p. 1-7.
22. Thirumavalavan, M., et al., *Cellulose-based native and surface modified fruit peels for the adsorption of heavy metal ions from aqueous solution: Langmuir adsorption isotherms*. Journal of Chemical & Engineering Data, 2010. **55**(3): p. 1186-1192.
23. Palaniappan, M., et al., *Synthesis and suitability characterization of microcrystalline cellulose from Citrus x sinensis sweet orange peel fruit waste-based biomass for polymer composite applications*. Journal of Polymer Research, 2024. **31**(4): p. 105.
24. Torres-Sciancalepore, R., et al., *Two-step valorization of invasive species Rosa rubiginosa L. husk waste through eco-friendly optimized pectin extraction and subsequent pyrolysis*. Journal of Environmental Chemical Engineering, 2023. **11**(5): p. 110802.
25. Nisar, J., et al., *Kinetics of pyrolysis of sugarcane bagasse: effect of catalyst on activation energy and yield of pyrolysis products*. Cellulose, 2021. **28**: p. 7593-7607.
26. Pravin Kumar, S.A., et al., *Thermogravimetric study and kinetics of banana peel pyrolysis: a comparison of 'model-free' methods*. Biofuels, 2022. **13**(2): p. 129-138.
27. Muhammad, F., et al., *Improved bio-oil yield from thermo-catalytic pyrolysis of Citrus limetta waste over pumice: Determination of kinetic parameters using Kissinger method*. Bioresource Technology Reports, 2023: p. 101635.
28. Nisar, J., et al., *Enhanced Bio-Oil Yield from Thermal Decomposition of Peanut Shells Using Termite Hill as the Catalyst*. Energies, 2022. **15**(5): p. 1891.
29. Varma, A.K., et al., *Investigation of kinetic and thermodynamic parameters for pyrolysis of peanut shell using thermogravimetric analysis*. Biomass Conversion and Biorefinery, 2020: p. 1-12.
30. Nisar, J., et al., *Kinetics of pyrolysis of sugarcane bagasse: effect of catalyst on activation energy and yield of pyrolysis products*. Cellulose, 2021. **28**(12): p. 7593-7607.
31. Lopez-Velazquez, M., et al., *Pyrolysis of orange waste: a thermo-kinetic study*. Journal of Analytical and Applied Pyrolysis, 2013. **99**: p. 170-177.



32. Zhang, B., et al., *Hydrothermal liquefaction of fresh lemon-peel: parameter optimisation and product chemistry*. *Renewable Energy*, 2019. **143**: p. 512-519.
33. Alvarez, J., et al., *Valorization of citrus wastes by fast pyrolysis in a conical spouted bed reactor*. *Fuel*, 2018. **224**: p. 111-120.
34. Westerhof, R.J., et al., *Effect of temperature in fluidized bed fast pyrolysis of biomass: oil quality assessment in test units*. *Industrial & Engineering Chemistry Research*, 2010. **49**(3): p. 1160-1168.
35. Miranda, R., et al., *Pyrolysis of sweet orange (Citrus sinensis) dry peel*. *Journal of Analytical and Applied Pyrolysis*, 2009. **86**(2): p. 245-251.
36. Nisar, J., et al., *Kinetics of the pyrolysis of cobalt-impregnated sesame stalk biomass*. *Biomass Conversion and Biorefinery*, 2020. **10**: p. 1179-1187.
37. Samolada, M., A. Papafotica, and I. Vasalos, *Catalyst evaluation for catalytic biomass pyrolysis*. *Energy & fuels*, 2000. **14**(6): p. 1161-1167.
38. Poddar, S., J. Ullas Krishnan, and J.S. Chandra Babu, *Non-catalytic and catalytic pyrolysis of citrus waste (orange peel)*. *Indian Chemical Engineer*, 2022: p. 1-28.
39. Afraz, M., et al., *Thermo-catalytic decomposition of cotton seed press cake over nickel doped zeolite Y, hydrogen: enhanced yield of bio-oil with highly selective fuel-range hydrocarbons*. *RSC advances*, 2024. **14**(43): p. 31549-31559.
40. Bhoi, P., et al., *Recent advances on catalysts for improving hydrocarbon compounds in bio-oil of biomass catalytic pyrolysis*. *Renewable and Sustainable Energy Reviews*, 2020. **121**: p. 109676.
41. Qiao, Y., et al., *Characterization of aroma active compounds in fruit juice and peel oil of Jinchen sweet orange fruit (Citrus sinensis (L.) Osbeck) by GC-MS and GC-O*. *Molecules*, 2008. **13**(6): p. 1333-1344.
42. Kravetz, C., et al., *Characterization of selected pyrolysis products of diseased orange wood*. *BioResources*, 2020. **15**(3): p. 7118-7126.
43. Al-Layla, N.M., L.A. Saleh, and A.B. Fadhil, *Liquid bio-fuels and carbon adsorbents production via pyrolysis of non-edible feedstock*. *Journal of Analytical and Applied Pyrolysis*, 2021. **156**: p. 105088.
44. Madhu, P., T.S. Livingston, and H. Kanagasabapathy, *Flash pyrolysis of lemon grass (Cymbopogon flexuosus) for bio-oil production in an electrically heated fluidized bed reactor*. *Waste and Biomass Valorization*, 2018. **9**: p. 1037-1046.
45. Volpe, M., et al., *Upgrade of citrus waste as a biofuel via slow pyrolysis*. *Journal of Analytical and Applied Pyrolysis*, 2015. **115**: p. 66-76.
46. Mishra, R.K., et al., *Thermocatalytic Pyrolysis of Waste Areca Nut into Renewable Fuel and Value-Added Chemicals*. *ACS Omega*, 2024.
47. Duku, M.H., *Bio-oil production from Lignocellulosic biomass using fast pyrolysis in a fluidized-bed reactor*. 2015.
48. Ji-Lu, Z., *Bio-oil from fast pyrolysis of rice husk: Yields and related properties and improvement of the pyrolysis system*. *Journal of Analytical and Applied Pyrolysis*, 2007. **80**(1): p. 30-35.
49. Thangalazhy-Gopakumar, S., et al., *Physiochemical properties of bio-oil produced at various temperatures from pine wood using an auger reactor*. *Bioresource technology*, 2010. **101**(21): p. 8389-8395.
50. Hosseinezhad, S., et al., *Physiochemical characterization of synthetic bio-oils produced from bio-mass: a sustainable source for construction bio-adhesives*. *RSC advances*, 2015. **5**(92): p. 75519-75527.
51. Zheng, J.-l., W.-m. Yi, and N.-n. Wang, *Bio-oil production from cotton stalk*. *Energy Conversion and Management*, 2008. **49**(6): p. 1724-1730.
52. Chukwuneke, J., et al., *Production and physico-chemical characteristics of pyrolyzed bio-oil derived from cow hooves*. *Arab Journal of Basic and Applied Sciences*, 2022. **29**(1): p. 363-371.
53. García-Pérez, M., A. Chaala, and C. Roy, *Vacuum pyrolysis of sugarcane bagasse*. *Journal of analytical and applied pyrolysis*, 2002. **65**(2): p. 111-136.



54. Abnisa, F., et al., *Utilization possibilities of palm shell as a source of biomass energy in Malaysia by producing bio-oil in pyrolysis process*. *Biomass and Bioenergy*, 2011. **35**(5): p. 1863-1872.
55. Amutio, M., et al., *Influence of temperature on biomass pyrolysis in a conical spouted bed reactor*. *Resources, Conservation and Recycling*, 2012. **59**: p. 23-31.
56. Xiu, S., A. Shahbazi, and R. Li, *Characterization, modification and application of biochar for energy storage and catalysis: a review*. *Trends in renewable energy*, 2017. **3**(1): p. 86-101.
57. Wang, W., et al., *Effect of nickel salts on the production of biochar derived from alkali lignin: properties and applications*. *Bioresource Technology*, 2021. **341**: p. 125876.
58. Li, C., et al., *Impact of heating rates on the evolution of function groups of the biochar from lignin pyrolysis*. 2021. **155**: p. 105031.



Data availability statements

The authors declare that the data are available in this manuscript in the form of tables and figures.

